ADDIS ABABA UNIVERSITY
SCHOOL OF GRADUATE STUDIES

GRAVITY STUDIES OF ERTA-ALE VOLCANIC RANGE, AFAR

BY

TEKETAY TSIGE GELAW

July, 2009

GRAVITY STUDIES OF ERTA-ALE VOLCANIC RANGE, AFAR

By

Teketay Tsige Gelaw

A Thesis Submitted to the School of Graduate Studies of the Addis Ababa University in Partial Fulfillment of the Requirements for the Degree of Masters of Science in Exploration Geophysics

Department of Earth Sciences

Addis Ababa University

June 2009

Addis Ababa

Addis Ababa University

School of Graduate Studies

GRAVITY STUDIES OF ERTA-ALE VOLCANIC RANGE, AFAR

By

Teketay Tsige

(Department of Earth Sciences)

Approved by Board of Examiners

_____	_____
Advisor	
_____	_____
Examiner	
_____	_____
Examiner	

ACKNOWLEDGEMENTS

Above all I would first and foremost like to praise the Almighty God for being on my side in all my endeavors with his endless love.

Next my deepest gratitude goes to different individuals, who had contributed a lot for the success of this thesis work. First I convey my warm and heartfelt thanks to my advisor Dr. Tilahun Mammo who has given me his constructive advice and guidance with understanding throughout the course of the study. Had it not been for his uninterrupted and genuine help, this research work would have not been accomplished.

Likewise, my families deserve special thanks beyond what words can express. They, during the time when they should get my assistance, have shared my pains and helped me in order for my dream came true. I can never forget your unreserved moral, understanding and concern.

My heartfelt deepest thanks also go to my wife Asmeret Moges who is always by my side sharing all ups and downs in my life.

I would like to express my special thanks to my friends Ato Mandefro Seyoum, Dessalegn Tekle, Taddese Meselu and Mebatsion Shawol for their moral and encouragement throughout my academic work.

Last but not least, Addis Ababa University, Department of Earth Sciences must be thanked for

funding the research. Thank you all!

Teketay Tsige

Abstract

An analysis of gravity data collected by the institute of Geological Survey of Ethiopia in conjunction with seismic wave velocity and Euler Deconvolution results to determine a preliminary crustal structure model of study area. The residual gravity anomaly indicates gravity maxima occur over magmatic segments and the gravity minima occur over the Ethiopian plateau escarpment and Danakil block which is related to low density material beneath the area. Gravity modeling using seismic wave velocity and Euler Deconvolution as a constraint indicates that the crust thins nearly 14.4Km over the study area. The presence of a thinned crust and higher density lower crust is characteristic of volcanic rifted margins. The study shows that the occurrence of geological structures, that are found the Ethiopian plateau escarpment, Erta Ale and Tat Ale volcanic range these structures are inferred from the high gradient residual gravity anomaly. In addition a significant thickness of sedimentary rock is observed in the beneath the study area.

TABLE OF CONTENTS

LIST OF FIGURES AND TABLES

CHAPTER 1

INTRODUCTION

1.1 Location of study area

Erta Ale area is in extreme northwestern part of Afar at latitude 13^{0}38’10.38’’ and longitude 40 37’39.39’’, with an average elevation of 231m from the WGS84 reference ellipsoid. Erta Ale has a NNW- SSE elongated caldera, with a subvertical rim scarp, hosting a lava lake. Erta Ale volcano lies along the on-shore Red Sea Rift (northern Afar, Ethiopia), separating the Nubia and Danakil plates.

Figure 1.1a Map of the study area**.**

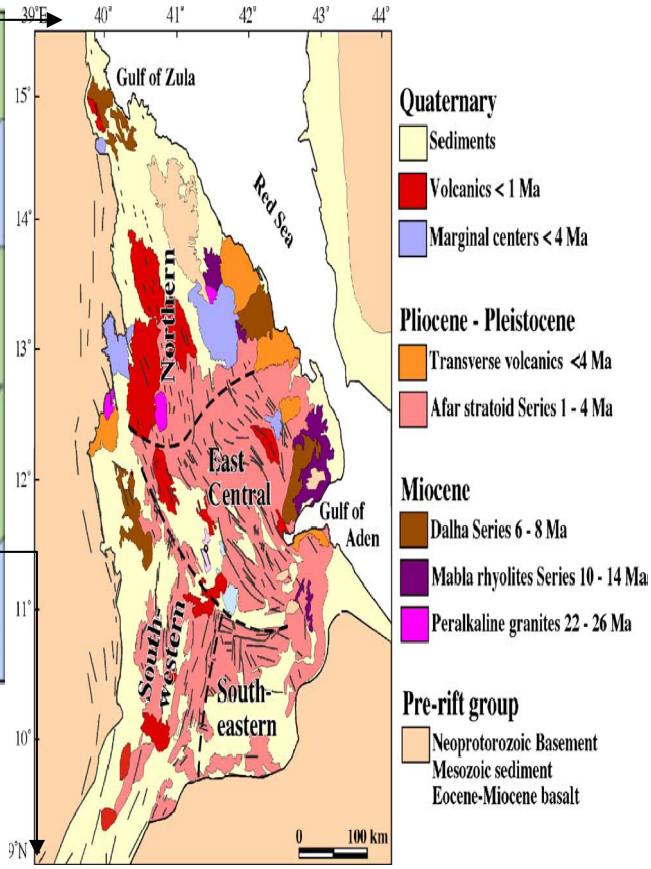

Figure 1.1b Geological map of the Afar Depression (after Varet, 1978; Acton et al., 1991).

1.2 Objective of the study

The main objective of this study was to understand the geologic and tectonic features which control Erta Ale volcanic range.

Under this objective the following specific objectives are set.

- Determining the tectonic feature of Erta-Ale.

- Mapping the layers beneath Erta-Ale.

- Producing 2.5D Model beneath the volcanic range.

1.3 Methodology

Geophysical investigations have been used to derive the structural and tectonic characteristics of large areas, play a major role in understanding the problems of the Earth crust. This study was conducted based on the gravity field, which is originated naturally within the earth due to gravitational sources. The gravitational field of the Earth is not uniform on the surface of the Earth, and its magnitude is measured by a Gravimeter, which is one of the most sensitive mechanical instruments. The purpose of the relative gravimeter is to measure the variation in main gravitational field of the earth that will later be used to infer the differences in rock density related to subsurface geologic structures. However, the interpretation of gravity using subsurface density variation is complicated by the fact that the variation in the gravitational field is not only by it, but also by other effects such as, the latitude of measurement (due to both Earth rotation and non-spherical shape), elevation, local topography, tides and instrumental drift. Therefore before interpreting gravity data to study the subsurface features, effects of the above mentioned cause must be removed from the measured gravity data. Even after removing the above mentioned effects the interpretation process is complicated by the fact that the reduced gravity data is still the superposition of the effect of the different subsurface density variations. Depending on the aim of the survey unwanted signal will be filtered out from the data to interpret the remaining signal to map the subsurface density variation.

1.4 Thesis structure

This thesis comprises of sex chapters. The first chapter deals about the location, objective and methodology. Chapter two consists and geological setting Chapter three consists of the theoretical frame work of gravity method for exploration. Gravity data and data processing are discussed in chapter four. Chapter five incorporates modelling and interpretation. Conclusions and recommendations are discussed in chapter sex.

1.5 Previous work

The gravity field of Ethiopia has been studied since the early 1960s (Gouin and Mohr, 1964; Mohr and Rogers, 1966) in order to determine the general crustal structure of the region the Afar region of northeastern Ethiopia (Makris et al., 1972; Mammo, 2004). The earlier studies (Makris et al., 1970, 1972; Searleand Gouin, 1972) determined that the MER and the northern Afar region coincided with a regional Bouguer gravity minimum that is related to crustal attenuation, while the southern Afar region is less attenuated and may contain continental crust. Although many geophysical and geological studies have been conducted in Afar depression crust, the nature of the crust below the region remains a topic of continuing debate. For example, using refraction seismic and gravity data, Makris and Ginzburg (1987) studied the crustal structure of the Afar depression, and suggested that the two crustal layers below Afar are thinned continental crust. They further argued that crustal thickness below Afar increases from 14km beneath the northern sector to 28km below the south segment of the depression, which is thicker than the crust below Iceland. Contrary to this view, Mohr(1989)suggested that the crust below the Afar depression is characterized by a new igneous material which has replaced the original bulk continental crust.

CHAPTER 2

GEOLOGICAL AND TECTONIC SETTING OF AFAR

2.1 Geology of the study area

The geological units of the Afar Depression and marginal areas can be divided into four broad groups.

(1) Neoproterozoic basement, Mesozoic sedimentary rocks, and Eocene–Miocene basalts

(2) Miocene igneous rocks

(3) Pliocene volcanic rocks

(4) Quaternary volcanic and sedimentary rocks.

1. **Neoproterozoic Basement, Mesozoic sedimentary rocks and Eocene–Miocene basalts**

The Neoproterozoic basement, which represents part of the Arabian–Nubian Shield, is prevalent on the periphery of the Afar Depression. The Arabian–Nubian Shield covers vast terrain to the north and northwest of the Afar Depression in eastern Eritrea and northern Ethiopia, respectively (Vail, 1985; Berhe, 1990; Stern, 1994).

The Neoproterozoic rocks of the Arabian–Nubian Shield also occupy parts of the Danakil and Ali-Sabieh Blocks.The Neoproterozoic basement rocks are overlain by Mesozoic sedimentary rocks that get progressivelyyounger towards the south and southwest on the Ethiopian and Somalian Plateaux, respectively. On the Ethiopian Plateau, the Mesozoic sedimentary rocks comprise Early Jurassic Adigrat Sandstone, Middle Jurassic Abay Limestone, Late Jurassic Antalo Limestone and Cretaceous Debre Libanos Sandstone. On the Somalian Plateau, the Mesozoic sedimentary rocks include Early Jurassic Adigrat Sandstone, Early Jurassic Hamanilei fossiliferous Dolomite and Limestone, Late Jurassic Urandab gypsiferous Limestone, and Early

Cretaceous Antalo Sandstones .The pre-rift group (Neoproterozoic basement/Mesozoic sedimentary rocks) either does not exist in the Afar Depression or are covered beneath the Pliocene and Quaternary volcanic and sediments. There are certain views regarding the influence of preexisting structures on the development of the Main Ethiopian Rift, the Red Sea and the Gulf of Aden. Many researchers have concluded that the structural and stratigraphic evolution of these structures have been significantly influenced by pre-existing Neoproterozoic faults, penetrative structures and terrane boundaries as in the case of the Red Sea and the Gulf of Suez (Almond,1986; Crane and Bonatti, 1987; Sultan et al.,1992; Montenat et al., 1998; Bosworth and McClay, 2001). However, few

researchers such as Mohr (1975) have argued that these rifts did not exploit pre-existing regional structural fabrics because the Main Ethiopian Rift run oblique to the nearest Neoproterozoic structural trends, the Red Sea obliquely cut the NNE-trending Neoproterozoic schist belt, and although older Neoproterozoic structures run parallel to the Sheba Spreading Axis other younger Neoproterozoic structures are orthogonal to the spreading axis. Within the Afar Depression, many structural features are found to suggest the influence of pre-existing fabric in its evolution. Black et al. (1974) identified the~900 km long pre-Miocene Marda Fault Zone, which continues from the Somalian Escarpment towards the Indian Ocean, to be in perfect alignment with the Red Sea western margin and the Erta Ale axial ranges. Purcell (1976) further proposed from gravity and seismic studies that the Marda Fault Zone is a major volcano-tectonic lineament aligned along the lithospheric weakness zone, that could be projected along the Erta Ale axial range to the Red Sea or along the Erta Ale axial range into the highlands of Eritrea where it corresponds with Neoproterozoic faulting and a significant facies change in the Jurassic limestone. Tectonism on the Marda Fault Zone itself is extinct, but it is still influencing the Pleistocene volcano-tectonic activities in the Afar Depression (Purcell, 1976). In addition, some isolated pre-rifting structural trends are located around the Afar Depression and could have local influence. Ghebreab (1998) and Ghebreab et al. (2002) identified N-trending Neoproterozoic shear zones at the northern tip of the Danakil Depression and further north along the Red Sea coast that were reactivated by younger structures. Collet et al. (2000) indicated reactivation of Neoprotorozoic structures that transect the western Afar margin, the Danakil Block and the western margin of the Arabian Plate.

The first known volcanism since the Neoproterozoic time appeared in northern Somalia and the first important volcanism occurred at the southern and western margin of the proto-Afar during the late Mesozoic (Mohr, 1975). The flood basalts of the Trap Series onthe African Plate covers ~500,000 km^2 and these are ~2000 m thick (Hofmann et al., 1997; Kazmin and Byakov, 2000). The Trap Series was extruded onto an erosional surface and sometimes found inter-bedded with fluvial, lacustrine and sub-aerial sedimentary rocks nearor above sea level (Civetta et al., 1975; Pallister, 1987;White and McKenzie, 1989).Berhe et al. (1987) have identified three stages of volcanismin the Trap Series at ~50–40, 40–30, and 30–21Ma whereas Ebinger et al. (1993) proposed that the main phase of volcanism occurred between 45 and30 Ma. Hofmann et al. (1997) concluded from 40Ar/39Arage dating in the Ethiopian Plateau that the Trap Series volcanic rocks were erupted over a short period of time at ~30 Ma.

2. Miocene igneous rocks

Eocene–Miocene flood basalts cover the Mesozoic sedimentary rocks on both the Ethiopian and the Somalian Plateaux and some parts of the marginal areas . Flood basalts of ~25–15 Ma found within the Afar Depression are deeply weathered and intensely faulted. These occur in limited area around the Gulf of Tajura and on the Ali-Sabieh Block (Varet, 1978; Vellutini,1990; Acton et al., 1991).Alkaline to per-alkaline intrusive rocks are found along the western and eastern Afar margins and the northern part of Afar (Figure 1.1b). These granites display clear intrusive contact with the Neoproterozoic basement, Jurassic Limestones and old Trap Series basalts (Varet, 1978). These are probably derived from mantle source as they have low Sr isotope ratio and might be associated with an early phase of continental break up (Barberi et al., 1972, 1974). Younger Miocene igneous rocks within the Afar Depression include the Mabla and Dalha Series (Figure 1.1b). The Mabla Series consists of rhyolites and ignimbrites with minor intercalation of basalts (Vellutini, 1990). These were erupted along N–S trending vents (Varet, 1978; Vellutini, 1990). The Dalha Series is a basaltic sequence up to 800 m thick found inter-bedded with rare detrital sedimentary rocks and ignimbrites (Varet, 1978).

3. Pliocene–Pleistocene volcanic rocks

Pliocene–Pleistocene volcanic rocks cover most of the Afar Depression (Figure 1.1b). They are by far the most important geological units in terms of coverage and preservation of igneous features and tectonic activities. The most significant series of these is the Afar Stratoid Series which is separated from Dalha Series by a nonconformity suggesting a prolonged erosion period and reduced magmatic activity (Varet, 1978). The Stratoid Series covers more than 2/3 of the Afar Depression. About 2/5 of these volcanic rocks are basalts frequently found to be porphyritic, vesicular, and tholeiitic in their geochemical nature (Barberi et al., 1974; Varet, 1978). The thickness of the Stratoid Series reaches up to 1500 m with individual flows varying from 1 to 6 m (Varet, 1978; Tefera et al., 1996).

4. Quaternary volcanic and sedimentary rocks

Quaternary volcanic rocks in the Afar Depression are composed of basaltic flows, scoria cones, and silicic rocks (Tefera et al., 1996). In most places basaltic fissure eruptions were followed by central eruptions that produced differentiates of basalt comprising alkaline and per-alkaline silicic rocks (Varet, 1978; Tefera et al.1996). However, the rift-parallel axial ranges (within the SE-propagating Manda Hararo–Gobaad and the NW-propagating Asal–Manda Inakir rifts) in the northern and east-central Afar are dominated by basalts which are ~1 Ma old. The Quaternary volcanic rocks, especially in the northern Afar are characterized by shield volcanoes .The axial ranges are forced along fissures showing symmetric magnetic anomalies that are underlain by thin oceanic-type crust,

and get progressively younger from the marginal zones towards the axial zones (Barberi and Varet, 1977). Because these show characteristics similar to mid-oceanic ridges, Barberi and Varet (1977) considered the axial ranges to be equivalents of oceanic spreading centers. E–NE trending volcanic centers transverse the NW–SE rifts found along the eastern and western Afar margins (Figure1.1b). These transverse volcanic centers are associated with fracture zones equivalent to oceanic fractures and composed of alkali basalts with inclusions of peridotite nodules indicating deeper mantle source (Barberi and Varet, 1975, 1977). Central volcanoes called marginal centers are also found in the Afar margins (Fig.2.1). These are characterized by the occurrence of summit calderas and are mainly composed of trachytic and rhyolitic rocks (Varet, 1978). Quaternary sedimentary rocks in the Afar Depression are dominated by lacustrine deposits. Significant lacustrine sedimentary rocks were deposited in the central Afar along the Manda Hararo–Gobaad rift zones between ~12 and 1 ka (Rognon, 1975). Lacustrine sedimentary rocks of ~180–200 m thickness cover the Awsa plain in the east-central Afar.

2.1 Volcano- Tectonics of Afar

The junction of Kenyan rift and Afar depression and its effect on the fault trends is clearly evident. Showing the characteristics of the triple junction with normal and sheared pattern of deformation (Courtillot, 1980).

In north Afar the early phase of the rift began between 25 and 23 m.y ago. This `phase features a climax in volcanic activities as well as geochemical change in the volcanic products. In the southern Afar, the initial phase of rifting cannot be clearly determined, probably beginning at approximately the same time as that of northern Afar.

The culmination of tectonic activity occurred between 9 to 11m.y. this tectonic phase known as choraro, is regarded as responsible for the present geological configuration of the southern Afar. The evolution of the graben was accompanied by the significant sinking, which becomes more intense moving northward.

A progressive process of crustal attenuation with transition from continental to an oceanic type of rift, characterize the transition from the northern Ethiopia to the Afar rift. Being the site of intense tectonic activity, with crustal thinning, Asthenosphere upraises and associated volcanism, both rift branches are certainly the site of the thermal regional anomaly. The associated of the observed

geothermal manifestation (hot springs, geysers, furmaroles) on the surface of both rift branches is clear illusion of the phenomena.

In of the southern part of Lake Abbe a very intense E-W fault belt extends eastward from the Wonjii fault belt. Up throws are dominantly to the south, but the variability permits the existence of a large graben in the north part of the E-W fault belt. A huge margin of this belt against the sediments of a once more extensive Lake Abbe. The E-W belt curves eastward to ENE-WNW trend (gulf of Aden), but becomes largely obliterated by ESE-WNW faults of the Djibouti republic , and indeed further south merges with this faulting. There is therefore no surface faulting extending inland WSW- wards from the of gulf Tajura directly towards the lake Abbe. Only south of latitude 11.140N (at the longitude of the gulf of Tajura) does weak Gulf of Aden appear.In south western Afar the north wards –flowing Awash River follows a narrow but widening belt between the Ethiopian plateau -Afar margin and the Wonjii fault belt (and its branch north from Amo-Issa). Indeed between Dofan volcano and Lake Hertale the Wonjii fault belt abuts against the plateau –Afar margin. North of Lake Hertale and the clearly expressed Ajelu –Amossa cross lineament, the faulting of Awash valley is of two trends : NNW-SSE parallel to the Ethiopian –Afar margin , and EWE-WSW as some linear and very persistent cross –rift lineament : the strongest of these cross rift lineament extend from Karakore east to the E-W fault belt immediately south of Lake Abbe.

The silicic centers of the Wonjii fault belt are situated where there is an inter section from a cross rift alignment, and their calderas or crater are elongated in the direction of the cross rift lineament. The Erta Ale volcanic range consists of several volcanic centers and fissural lava fields. Bounded on all sides by recent evaporitic deposit, this volcanic range extends from the Salt pain to the north to the Gilietti Lake to the south, reaching more than 100km in length and 20 to 30km in width, covering an area of about 2500km^2. The Erta Ale volcanic range is the largest volcanic unit of the Northern Afar and occupies the median part of the depression.

CHAPTER 3

GRAVITY FIELD OF THE EARTH

3.1 Introduction

Gravity and magnetic field are two natural forces fields interact to earth. This is because the earth has the ability to attract material masses towards its center. Gravity field is always an attractive force.

The earth also attracts or repels material which has a magnetic property (Telford, et al, 1990).

The fundamental principle of the gravity method is based on the Newton's law of gravitation. It states that every particle of matter exerts a force of attraction on every other particle this force is being directly proportional to the product of the masses and inversely proportional to the square of the distance between them.

$$F=G\frac{m_1 m_2}{r^2} \tag{3.1}$$

where F – is the attractive force between two masses of mass m_1 and mass m_2.

r- is the mean distance between two masses.

G- is the universal gravitational constant which has a value of

$6.672\text{x}10^{-11}\text{Nm}^2/\text{kg}^2$.

According to Newton's second law this force can be an external force exerted by one body to another body that can cause a change of state to this body.

Mathematically:

$$F_{12}=G\frac{m_1 m_2}{r^2} = m_2 a_2$$

and

$$F_{21}=G\frac{m_1 m_2}{r^2} = m_1 a_1$$

where F_{12} is the force exerted by m_1 on m_2 and F_{21} is the force exerted by m_2 on m_1.

Typical example - A mass m above the earth of mass M will be attracted by:-

$$F=G\frac{Mm}{r^2}=m\mathrm{g}$$

$$\frac{F}{m}=G\frac{M}{r^2}=\mathrm{g} \qquad (3.2)$$

where g- is gravitational field intensity or intensity of gravitational acceleration.

Gravity: is the force per unit mass to accelerate the mass m on the surface or exterior of the earth. Gravity field can have components along x, y and z. in this case we call it the gradient field.

$$\text{grad g}=\nabla \mathrm{g}=\frac{\partial g}{\partial x}+\frac{\partial g}{\partial y}+\frac{\delta g}{\delta z} \qquad (3.3)$$

Measuring the gravity field of the earth is position dependant i.e. g=g(x,y,z) where x, and z represents latitude longitude and height respectively or g=g(r,θ,φ) in spherical coordinate.

$$\mathrm{g}=G\frac{M}{r^2}$$

Unit of g in Geodesy is Gal [G] given in the honor of Galileo Galilee.

$$1\text{Gal}=1\text{cm/s}^2=10^3\text{mGal}.$$

Gravity unit (g.u)

$$1\text{g.u}=0.1\text{mGal},\ 1\text{Gal}=10^3\text{mGal}$$

The units tell you the accuracy of determination. The smallest unit has more precision than the big unit.

3.2 Gravitational potential

Gravity field can be represented by a scalar quantity called the gravitational potential. The gravitational potential, energy $U(R)$, is defined as the work done by a gravitational force to move a point mass from a very distant point (mathematically from infinity) by any path at all to a point distant, R, from the centre of gravity of M, It is given by:

$$U(r) = \int_{\infty}^{R} g.\,dr = -GM\int_{\infty}^{R}\frac{dr}{r^2} = \frac{GM}{R} \qquad (3.4)$$

Since the gravitational potential energy is a scalar quantity it is easier to determine the gravitational acceleration vector from the potential as:

$$F(r)m = g(r) \qquad (3.5)$$

As can be seen from the above equation g can be expressed in terms of a potential, U, therefore, gravity exploration is referred to as a potential – field technique.

Moreover, in gravity exploration we account only the vertical component of the gravity field gz because it is the only direction in which g can be measured directly (Telford, et al 1980).

3.2.1 Three dimensional (Newtonian) potential

The potential at a point some distance r away from a three dimensional mass which has arbitrary shape can be calculated by first dividing the mass in to small element of mass dm and latter integrating it in order to get the total effect.

The potential of an element mass dm at a distance r from the centre of mass is:

$$dU = G\frac{dM}{r} = G\sigma\frac{dx\,dy\,dz}{r} \qquad (3.6)$$

where,

σ = density

$r = (x^2+y^2+z^2)^{1/2}$

Therefore, the potential of the total mass M is found as:

$$U(x,y,z) = G\sigma\int_x\int_y\int_z\frac{1}{r}\,dx\,dy\,dz \qquad (3.7)$$

In cylindrical coordinates,

$dv = r\,dr\,d\varphi\,dz$, the u (r, φ, z) is :

$$U(r, \varphi, z) = G\sigma \int_r \int_\varphi \int_z dr\, d\varphi\, dz \tag{3.8}$$

In spherical coordinates,

$$dxdydz = r^2 \sin\theta\, dr\, d\theta\, dz,$$

Hence the potential in spherical coordinates will be,

$$U(r, \theta, \varphi) = G\sigma \int_r \int_\varphi \int_\theta r \sin\theta\, dr\, d\varphi\, d\theta \tag{3.9}$$

Since the gravity field can be derived from the scalar gravitational potential then, the acceleration in the vertical (Z) direction which is the only component of g that can be measured directly will be,

$$G_z = \frac{\partial U}{\partial Z} \tag{3.10}$$

In Cartesian coordinate system,

$$g_z = -G\sigma \int_x \int_y \int_z \frac{Z}{r^3}\, dx\, dy\, dz$$

In Cylindrical coordinate system,

$$g_z = -G\sigma \int_r \int_\varphi \int_z \frac{Z}{r^2}\, dr\, d\varphi\, dz \tag{3.12}$$

In Spherical coordinate system,

$$g_z = -G\sigma \int_r \int_\varphi \int_\theta \sin\theta \cos\theta\, dr\, d\varphi\, d\theta \tag{3.13}$$

Note: In the above equations (3.11, 3.12 and 3.13) the density assumed to be constant throughout the volume.

3.2.2 Two dimensional (logarithmic) potential

Consider a two dimensional body which has arbitrary shape. If the mass is very long in the Y – direction and has uniform cross section in the XZ plane, then the gravity attraction derives from a logarithmic potential.

The logarithmic potential expression becomes:

$$U(x,z) = 2G\sigma \int_X \int_Z \log\frac{1}{r}\, dx\, dz \qquad (3.14)$$

Therefore, the gravity effect of the two dimensional body will be:

$$g_z = \frac{\partial U}{\partial Z} = -2G\sigma \int_x \int_z \frac{z}{r^2}\, dx\, dz \qquad (3.15)$$

Where, $r = (x^2 + z^2)^{1/2}$ This equation is used for calculating the gravity effects of bodies of uniform density and regular shape such as, sphere, cylinder, horizontal slab etc.

3.3 Geometry of the gravity field

3.3.1 Gravity of a rotating sphere

Consider a small mass moving with a velocity v on the surface of the earth rotating with angular velocity ω as shown below. T

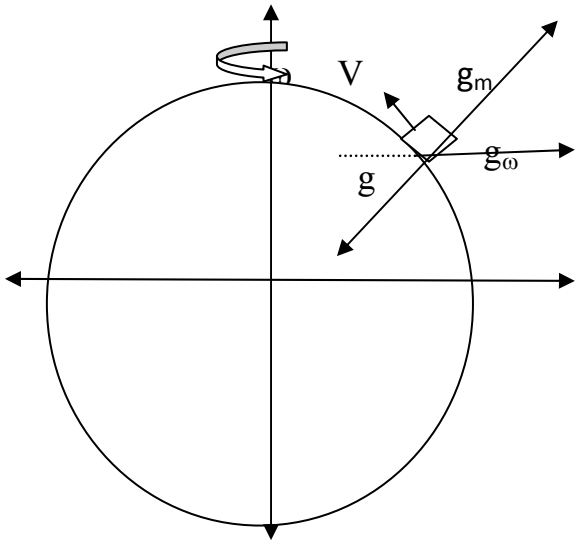

Figure 3.1 Force components affecting g_m

The possible force acting on a body of mass m moving with a velocity v on the surface of the spherical Earth of radius R rotating with angular velocity ω are:

$g = g_m + g_\omega + C + T$ and is known as gravity.

where g_m– is the attraction force per unit mass acting on m due to Earth's mass.

g_ω– is the centrifugal force per unit mass acting on m due to Earth's rotation with ω.

C– is the coriolis force per unit mass acting on m due to its motion with linear velocity v on the earth of the earth.

T – is the tidal force per unit mass acting on m due to mass attraction of other heavenly bodies.

For spherical model of the earth with radius R:

$g_m = G\frac{M}{R^2}$; $g_\omega = \omega[\omega x R]$, $F\omega = m\,\omega[\omega x R]$

$C = 2[\omega x v]$; C=0 if v=0 or if m is at rest on the surface of the earth.

It is not easy to express T with a simple formula due to the variation in position [as they are always rotating their position change with respect to position of m] and a number of heavenly bodies causing it.

The effect of C and T on g is usually considered negligible in actual work; g refers to the combined effect of both Earth's mass gravitation and rotation [centrifugal acceleration] i.e.

$$g = g_m + g_\omega$$

$$g = G\frac{M}{R^2} + \omega[\omega x R] \qquad (3.16)$$

3.3.2 The earth's figure and gravity

The elliptical shape of the earth with the widest portion of the ellipse aligning with the equator was first proposed by Isaac Newton in 1687.

The shape of the Earth and gravity has a close relationship. The shape of the Earth is distorted from a spherical shape this is due to its rotation. The best mathematical approximation to the figure of the earth is an oblate ellipsoid this can be referred as the International Reference Ellipsoid.

The dimension of the reference ellipsoid has been refined continually as more exact data have become available. In 1980 at the International Union of Geodesy and Geophysics (IUGG) geodesists and geophysicists agreed to take ellipsoid that has equatorial radius (a), 6378.136 km and polar radius (b), 6356.751 km, as a reference Ellipsoid GRS80. Where as the radius of the equivalent sphere is 6371.000 km.

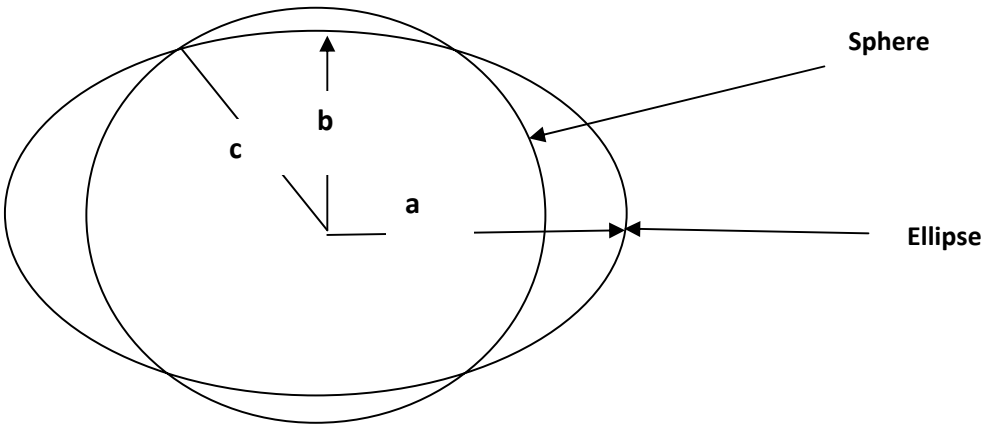

Figure 3.2 Comparison of the dimensions of the international reference ellipsoid of 1980, with a sphere of equal volume.

The polar flattening (f) is defined as:

$$F = \frac{a-c}{a} \tag{3.17}$$

The surface of the ellipsoid is to be a level surface in the normal gravity field (Torge, 1989). The earth's gravity potential (W) on the surface of the earth consists of the mass gravitational potential (U_m) and the centrifugal potential (V_Φ).

The centrifugal potential arises from the radial component of the centrifugal acceleration.

Therefore,

$$W = U_m + V_\varphi \tag{3.18}$$

$$W(X,Y,Z) = G\iiint \sigma \frac{dy}{z} + \frac{1}{2}\omega^2 (X^2 + Y^2) \quad (3.19)$$

The relationship between gravity and gravity potential is:

$$g = \text{grad } W \quad (3.20)$$

3.4 Equipotential surfaces and plumb lines

The gravity field can be geometrically described by surfaces of constant gravity potential (Equipotential surfaces, level surfaces)

$$W(r) = \text{const.}$$

and by plumb lines. The relationship between changes in potential and changes in position follows from the relation, g = grad W.

$$\text{i.e.} \qquad dW = g.dr = gdr\cos(g,dr) \quad (3.21)$$

If a test mass is moved along a level surface, we have dW = 0. As a result no work is performed; the level surfaces are equilibrium surfaces.

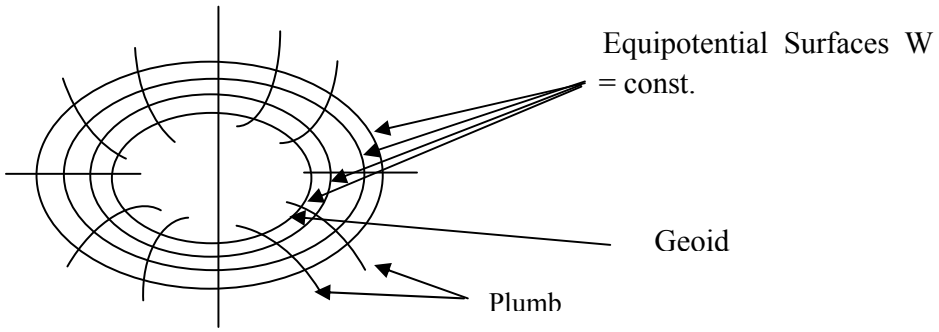

Figure 3.3 Equipotential surfaces and plumb lines near the Earth's Surface.

The plumb lines intersect the level surfaces perpendicularly.

Differentiating the gravity potential W = W(x,y,z), we will get,

$$dW = \frac{\partial W}{\partial X}dx + \frac{\partial W}{\partial Y}dy + \frac{\partial W}{\partial Z}dz \quad (3.22)$$

If the vector ds is taken along the Equipotential surface W = Wo, then the potential remains constant and dW = 0. $\text{i.e.} dW = \text{grad}W.ds = g.ds, \text{then } g.ds = 0$ (3.23)

Since gravity varies due to factors such as variation in mass distribution, the level surfaces are not parallel. The level surface which approximates mean sea level is denoted as geoid. It serves as a reference surface for defining height systems (Torge, 1989).

Geoid is defined as an equipotential surface corresponding with mean sea level surface. The mean sea level is considered because the oceans are subject to tides and currents. For practical work, measurements of gravity is carried on the physical equipotential surface i.e. geoid or on its best approximation, the ellipsoid.

The theoretical value of gravity $\gamma\Phi$ on the rotating ellipsoid can be computed by differentiating the gravity potential W and thus,

$$g_{\varphi} = \text{grad}W \tag{3.24}$$

If we considering a rotating ellipsoid W will be the potential due to the attracting mass and rotation. Making the necessary mathematical treatment we will arrive at the variation of the theoretical gravity value γ_{Φ} that is normal to the ellipsoid surface. This value is given as:

$$\gamma_{\varphi} = \gamma_{e}\,(1 + \beta\sin^{2}\Phi - \beta_{1}\sin^{2}2\Phi) \tag{3.25}$$

Table 3.1 Normal Gravity Formulas (Torge, 1989).

Name	γe	B	β1	f
HELMERT (1901)	9.78003	0.005302	0.000 007	1:298.3
U.S.Coast and Geodetic Survey (BOWIE 1917)	9.78039	0.005294	0.000007	1:297.4
International Gravity Formula (CASSINIS 1930)	9.78049	0.0052884	0.0000059	1:297.0
Geod. Ref. System 1967 (INT. ASS. GEOD. 1971	9.780318 (incl. atmosph. mass)	0.0053024	0.0000059	1:298.247
Geod. Ref. System 1980 (MORITZ 1984)	9.780327 (incl.atmosph. mass)	0.0053024	0.0000058	1:298.257

Where, γe is the value of gravity at the equator Φ = 0, β = gravity flattening and β1 is computed from the flattening *f* and the ratio of equatorial centrifugal acceleration and equatorial gravity (m).

The mathematical formula used to predict the components of the gravitational acceleration produced by the earth's shape and rotation is called the Geodetic Reference Formula. The predicted gravity is called the normal gravity.

The formula for calculating the normal gravity γΦ at any latitude, Φ, on a rotating ellipsoid was revised in 1967 by the International union of Geodesy and Geophysics (IUGG). Incorporating the parameters;

Re = 6,378,160 meters

Rp = 6,356,774.5 meters

f = 1/298.247

ω = 7.2921151467 x 10^{-5} radian/second

γe = 978.031846 gals

in the normal gravity formula, $\gamma\Phi = \gamma e\ (1 + C_1 \sin 2\Phi + C_2 \sin 4\Phi)$, where, the constants C_1 and C_2 depend on the flattening *f* and the rate of rotation ω. We will get;

$$\gamma_\Phi = 978.031846(1 + 0.005278895 \sin^2\Phi + 0.000023462 \sin^4\Phi) \quad (3.26)$$

The above equation is called the 1967 Geodetic Reference System (GRS67) formula (Robinson, 1988).

The normal gravity formula (γe) that was used as a reference for our gravity data reduction is the Geodetic Reference System, GRS80 formula by (Moritz, 1984).

$$\gamma_{\varphi(1980)} = \gamma_e \frac{1 + \kappa \sin^2 \varphi}{(1 - e^2 \sin^2 \varphi)^2} \quad (3.27)$$

where, γe = 9.7803267715 ms^{-2}

κ = b γp/ a γe - 1 = 0.001 931 851 353

$e^2 = a^2 – b^2 / a^2$ = 0.006 694 380 0229

3.5 Gravity Reference Systems

Since spring gravimeters measures the relative gravity values between observation sites, it is important to find the absolute gravity values at the observation point. In order to determine the absolute gravity value at the observation point at least one gravity base station is needed, where its absolute gravity value is known.

The absolute gravity value at each station can be determined by tying it with the global reference system, the International Gravity Standardization Net, 1971(I.G.S.N.71) (Morelli et al, 1974).

Hence, the absolute gravity (g) value at the observation site can be found by;

$$g = g_r + \Delta g \tag{3.28}$$

where, g_r is the absolute gravity value at the base station; Δg, the gravity difference between the base station and the observation site after corrected for, tied and drift. (Robinson et al, 1988).

3.6 Gravity reductions

In gravity surveys, field work is carried on land by taking gravity readings on a profile, at grid stations or scattered points covering an area of interest with station interval that takes into consideration the frequencies of interest to be observed. In all gravity surveys the vertical component of g, g_z, is measured. A gravity survey shows variation in the g_z reading which is caused by, instrumental drift, earth tides, local topography or terrain, and variation in subsurface density. Therefore, in order to see the desired anomaly which is caused by variations of subsurface density, it is important to correct the other non – geologic factors that affect the value of g_z. In general all gravity values are reduced to a datum plane, but this plane need not necessarily be the sea – level surface (Dobrin, 1988). Those factors which affect the gravimeter readings are classified as temporal and spatial variations.

3.6.1 Temporal variations

The temporal variation includes the time varying factors: namely instrumental drift, tare and tidal effects, and pressure effect.

3.6.1.1 Drift and Tare correction

Instrumental drift is the time dependent mechanical changes within the gravimeter even though the gravimeter is handled with care. These variations in the gravimeter spring properties with time can be due to stretching of the spring, associated with temperature and/or pressure changes. Instrumental drift results on that repeated observations at one location yield different values for the gravitational acceleration. The gravimeter is usually read more times a day for several days. To correct the change in gravimeter reading that is caused by instrumental drift or tare, the usual practice is to reoccupy one or more stations periodically during a gravity survey. Repeated gravity readings at one station will give a series of different gravity values, which is useful to produce a drift curve for the instrument. In order to determine drift effect properly, we should make gravimeter readings at one to three hour intervals (Robinson, 1988).

Another unwanted and more serious problem that needs a special treatment is the tare effect. A tare occurred due to an abrupt change in the gravimeter reading. Gravity variation of several tenths of mGal or more may occur due to tare effect (Robinson, 1988). Repeated reading at one or more stations and a careful analysis of the drift before and after the tare effect is needed to remove its effect from measurements.

In high precision surveys measurements will be taken repeatedly in more than one point and adjustment of measurements will be carried out using computer programs aided with visual control of tare effects (Becker, 1984).

3.6.1.2 Tide correction

Tides are caused by variations in gravity observations resulting from the attraction of the celestial bodies (moon and sun). The Earth's body experiences an elastic deformation due to the tidal forces (earth body tides) (Torge, 1989). The resulting bulges in the surface have diurnal periodicity which is predictable at any point on the surface of the Earth. The tidal variations can be on the range of 0.2 to 0.3 mgal (Dobrin, 1988). So to use the full sensitivity of the gravimeter these variations must be removed.

In some small scale surveys it may be reasonable to assume that the tidal variations are linear with time during the intervals between the times that a base or reference station is reoccupied. In this case the tidal variations are included and treated in the same manner as the slow drift in gravimeter readings caused by inherent strain in the sensing element.

The tidal variation of gravity which is obtained by a gravimeter survey can be corrected based on the masses of the sun and moon and their positions relative to an observation site. This can be computed by the formula:

$$\delta g_T = \frac{3}{2}\sigma GR\left[\frac{M_m}{r_m^3}\left(\cos 2\theta_m + \frac{1}{3}\right) + \frac{M_s}{r_s^3}\left(\cos 2\theta_s + \frac{1}{3}\right)\right] \quad (3.29)$$

where, R, is the earth's radius, Mm and Ms are the lunar and solar masses and their distances from the earth s centre are r_m and r_s. The value $\sigma = 1.16$ accounts for the way that the earth itself is stretched elastically by the tidal force. Angles θ_m and θ_s between a line from the earth's centre to the observation site and lines from the earth's centre to the moon and sun change with time. These formulas are long and complicated; a computer program is ordinarily used to make the calculations (Robinson, 1988).

A more accurate way of removing the tidal effect is through the usage of tidal models such as Dodson, Cartwright etc (Torge, 1989).

3.6.2 Spatial based variations

These are changes in the observed gravitational acceleration that are space dependent. Just like the geologic effects, these change the gravitational acceleration from place to place, but these are not related to the subsurface geology.

3.6.2.1 Latitude Correction

If the earth were a homogenous non-rotating sphere with the same vertical gradient everywhere, apart from local near surface density variations due to geological structures, and if it were a perfectly smooth surface, then clearly all gravity variations over the surface would be caused by geological structure. But this is not so. Because of the flattening, the poles are near to the center of mass than the equator, so that the gravity increases with increasing in latitude. The variation of gravity with latitude over the surface of an ellipsoid earth can be expressed by the revised theoretical gravity formula estimated by IAG in 1967.

The latitude correction $\delta\gamma_\phi$ is obtained by differentiating;

$$\gamma\phi_{1967} = 978031.85\left(1 + 0.0053024\sin^2(\phi) - 0.0000059\sin^2(2\phi)\right)\text{mGal} \quad (3.30)$$

with respect to ϕ and is added to g as we moved towards the equator, i.e,

$$\delta\gamma_{\phi}\int\frac{\phi}{ds}=\left(-\frac{1}{R}\right)\frac{\delta\gamma_{\phi}}{\delta\phi}/\delta\phi=0.811\sin 2\phi \text{ mgal /km} \tag{3.31}$$

where R is the radius of the earth R =6371km, s=R =N_S horizontal distance, and ϕ is latitude angle.

3.6.2.2 Free – Air correction (δgF_A)

In this case, the topographical masses above mean sea level (datum) surface up to the observation point is ignored. The observation point is thought as if it is suspended in the air and, hence the name free – air. In changing elevation, gz, changes because of the change in distance from the centre of mass of the earth up to the gravity observation point. Therefore, it is necessary to correct for changes in elevation between stations. As a result all field readings are reduced to a datum surface.

From Newton's law we have that,$g_z = G\frac{M_e}{R_e^2}$ differentiating this equation with respect to Re we will get the value of the free air correction as:

$$\delta g_{FA}=\frac{dg_{FA}}{dR_e}=-\frac{-2M_e}{R_e^3}\approx-\frac{2g}{R_{eq}}\approx-\frac{0.3086\text{mgal}}{\text{m}} \tag{3.32}$$

where, δg_{FA} is the free air correction and Req is the equivalent radius.

As the negative sign implies, the free – air correction is added to the field reading when the station is above the datum plane and subtracted when below it. In order to apply free – air correction the station position must be precisely known. .

Note: If the gravity measurement accuracy is about 0.01 mgal, which is the sensitivity of the most of the present day gravimeters, then we must know our elevation to 2 inches (5.08cm) (Telford et al, 1990).

3.6.2.3 Bouguer correction (δg_b)

The Bouguer correction is a correction to account for the excess mass underlying observation points located at elevations higher than the elevation datum (sea level or the geoid). Conversely, it accounts for a mass deficiency at observation points located below the elevation datum. The two assumptions that are useful in deriving the Bouguer correction are, the slab is made of uniform density and it has infinite horizontal extent. As one changes elevation there are changes in g caused by the added (or

subtracted) layer of material that has been included. Thus in moving up from a valley to a plateau the gravity decreases due to the increasing distance from the centre of mass but it also increased by the attraction of the slab of rock whose thickness is the change in elevation.

The gravitational attraction of an infinite slab of thickness Δz and density σ is:

$$\delta g_B = 2\pi G \sigma \Delta z = 0.04193 \sigma \Delta z \quad (3.33)$$

where σ is in gm cm-3, Δz is in meters and δgB is the Bouguer correction. (Robinson et al, 1988). If we assume that the slab has density of 2.67 gm cm-3, the Bouguer correction will be δg_B = 0.1118 mgal /m.

The effect of this intervening slab is called the Bouguer effect and the correction is called Bouguer correction. It is the opposite sign to the free air correction. This effect may be difficult to calculate because one does not know the density. Furthermore, if the elevation change is confined to a small region, like going up a hill, then the infinite slab is an inappropriate description of the intervening mass. Under this circumstance the actual topography must be considered and another effect, the terrain effect, is included. Conventional practice is to apply the Bouguer correction first and, the terrain correction.

3.6.2.4 Terrain correction (δg_t)

The Terrain correction accounts for variations in the observed gravitational acceleration caused by variations in topography near each observation point. With considerable topographic relief the infinite Bouguer slab is not a good model for the intervening mass between the reference elevation and the point of observation. The actual gravitational effects must be calculated numerically for the masses above and below the slab surface.

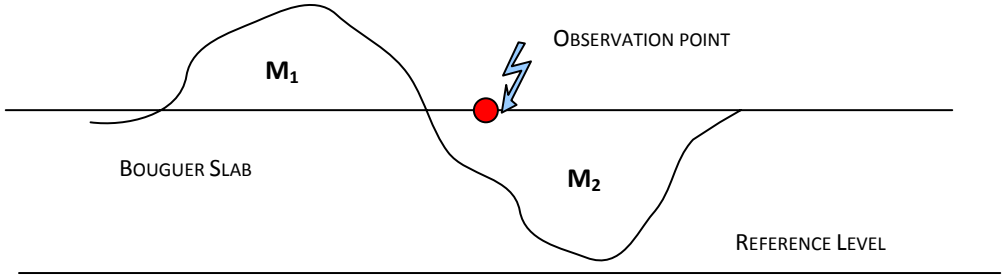

Figure 3.3 Topographic effects of the valley (M_2) and the mountain (M_1) on the gravity observation point.

In the above figure (3.3), M_1 is a mass excess adjacent to the observation point which reduces the value of g_z. M_2 is a mass deficit adjacent to the observation point which also reduces the value of g_z. Similar to the Bouguer reduction it is necessary to determine the appropriate density values of the surrounding lithologic units to carry out terrain reduction. The terrain corrections are difficult to do in very rugged terrain because the nearest features have the biggest effect. Choosing the density is also a problem but an iterative process is used until the corrected data shows no correlation with the topography.

When the terrain in the vicinity of the observation point is rugged, the whole area is represented by concentric circles and radial lines, making sectors whose areas increase with distance from the centre. The gravity effect of a single sector can be calculated from the formula:

$$\delta gt\,(r,\theta) = \sigma G\theta \left\{ \left(r_o - r_i\right) + \frac{\left(r_i^2 + z^2\right)}{2} - \frac{\left(r_o^2 + z^2\right)}{2} \right\} \qquad (3.34)$$

where; θ = sector angle (radians), z = les – lea, es = station elevation, ea = average elevation in sector, r_O, r_i = outer and inner sector radii respectively (Telford, et a, 1990).

The terrain correction is the sum of all the sectors. Therefore, if we have n number of sectors, the total terrain correction will be:

$$\delta g_T = n\,\delta gt\,(r,\theta) \qquad (3.35)$$

Now a day, it is customary to model the topography of the survey area and its surrounding using parallelepipeds (Nagi, 1966; Banerjee and das Gupta, 1977) and compute the effect of each parallelepiped at measurement points to carry out terrain reduction.

Because of the assumptions made during the Bouguer Slab correction, the terrain correction is positive regardless of whether the local topography consists of a mountain or a valley region. As a result the terrain correction is always added to the station reading.

3.7 Gravity anomaly

The word anomaly implies deviation from the normal. Gravity anomalies (Free – air and Bouguer) are geophysical tools up on which effects of geology on the earth's gravity field can be detected.

If g_{obs} is the measured gravity value at station elevation h above the geoid, it should be reduced to sea level (geoid) to compare it with g_{Φ}, the theoretical value on reference ellipsoid of the same latitude Φ. Therefore the gravity anomaly at a station is defined by,

$$\Delta g = g_{obs} - \gamma_{\Phi}$$

where; Δg is the gravity anomaly; gobs is the measured gravity value of a station reduced to geoid surface, after the temporal and spatial corrections have been applied; γΦ, the theoretical gravity of the station at latitude, Φ.

In order to get the desired anomaly that is caused by geologic structure, we have to correct the measured gravity value, for the corrections that we have mentioned before. Therefore:

The Free - air anomaly (ΔgFA)

$$\Delta g_{FA} = g_{obs} + 0.3086h - \gamma_{\Phi(1980)} \text{ (mgal)} \quad (3.36)$$

Where, h is the elevation at which the gravity station is above the datum chosen for the survey.

The Bouguer Anomaly (ΔgB)

$$\Delta g_B = g_{obs} + 0.3086h - 0.04193\,\sigma\,\Delta z - \gamma_{\Phi(1980)} \text{ (mgal)} \quad (3.37)$$

The Terrain Corrected Bouguer Anomaly (ΔgT)

$$\Delta g_T = g_{obs} + 0.3086h - 0.04193\,\sigma\,h + \delta g_T - \gamma_{\Phi(1980)} \text{(mgal)} \quad (3.38)$$

Note: Considering that the above corrections have accurately accounted for the variations in gravitational acceleration they were intended to account for, any remaining variations in the gravitational acceleration associated with the Terrain Corrected Bouguer Gravity Anomaly, Δg_T, can now be assumed to be caused by geologic structures.

CHAPTER 4

GRAVITY DATA AND DATA PROCESSING

4.1 Gravity data

The gravity data used for this study were obtained from Ethiopian Institute of Geological Survey (EIGS). These data set consists of 305 gravity points (Figure 4.1) and all the stations were tied to IGSN71 (International Gravity Standardization Net 1971; Morelli et al., 1971), which is located in Addis Ababa.

4.2 Analysis of gravity signals

All the gravity data were reduced by making fundamental corrections, including drift, latitude, free air and terrain corrections. The observed gravity values were reduced to sea level using a uniform crustal density of 2.67 g/cm^3. The Bouguer and free- air gravity anomalies were calculated using the Geodetic Reference System of 1967(GRS67). After all the reductions have been made the data was analyzed by using two-dimensional extrapolation followed by two-dimensional smoothing of the noise introduced by the extrapolation, and extracting one-dimensional profiles from the smoothed two-dimensional contour maps is carried out by using SURFER 8 mapping software.

4.2.1 Bouguer anomaly

The Bouguer contour map has been produced based on a geostatic gridding method called Kringing with a contour interval of 5mGal so that the short and long wavelength anomalies may be separated out in Figure 4.2.

The resulting map characterized by the gravity anomaly varies between -140mGal to 20 mGal. The Bouguer anomaly map indicates high gravity anomaly is dominated in NNW-SSE trending which might be associated with the Erta Ale and Tat Ale Axial volcanic ranges and this indicates either the intrusion of high-density material into the crust or the thinning of the crust. In contrary, highly negative values are observed over the Ethiopian plateau which is related to thinning of the mantle lithosphere has been occurred below this region.

In general a prominent gravity low indicates depression in the basement or low density volcanic material on the surface or low density upper mantle material beneath the surface.

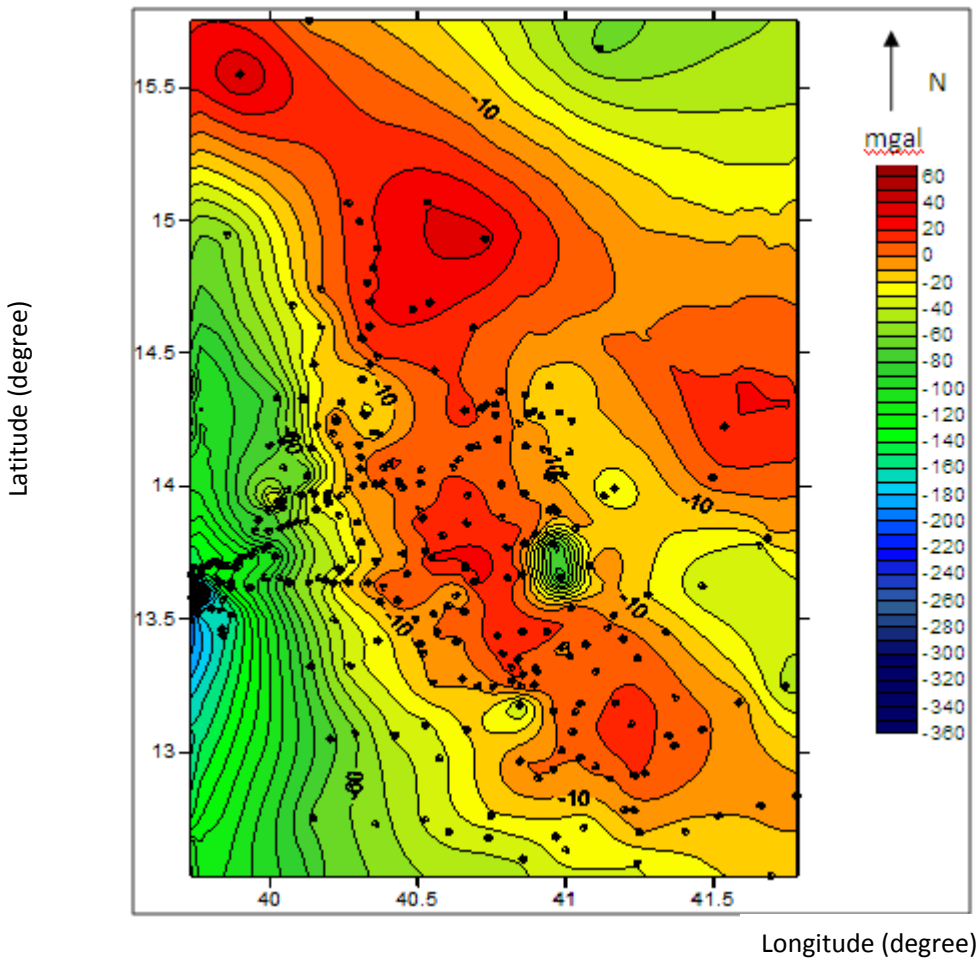

Fig 4.2 Bouguer Anomaly map

4.2.2 Regional-Residual separation

In order to produce gravity anomalies of local and regional origin, a regional – residual separation method of 3rd order polynomials fitting is applied to the Bouguer anomaly.

4.2.2.1 Residual anomaly

Since the regional gravity field has been removed out from the Bouguer gravity, the only effects expressed in the residual gravity map are those caused by the local geology. The correlation between the residual anomalies and the local geology along the volcanic range is very clear. The residual anomaly map indicates high gravity anomaly is dominated in NNW-SSE trending and the rest of the region, the Ethiopian Plateau and Danakil block, is filled with negative residual anomaly. Even though these regions are covered with high density material, they exhibited negative residual gravity anomaly this might be an indication of the existence of some geological structures (bodies) which

attributed to very low density beneath the surface. This will agree with (Mohr, 1967a) the northern part of the Danakil horst is composed of Precambrian basement rocks overlain by Mesozoic sedimentary rocks similar to those on the Ethiopian Plateau.

Comparison of the residual anomaly map (Figure 4.3) with geological map (Figure 1.1b) shows the positive correlation between gravity high and active faulting and magmatic centers. For example, high gravity anomaly coincides with Erta- Ale and Tat Ale volcanic range, indicating a crustal thinning is occurred in these regions where dense material intrudes the overlaying crust and the area is overlaid with Pliocene flood basalt.

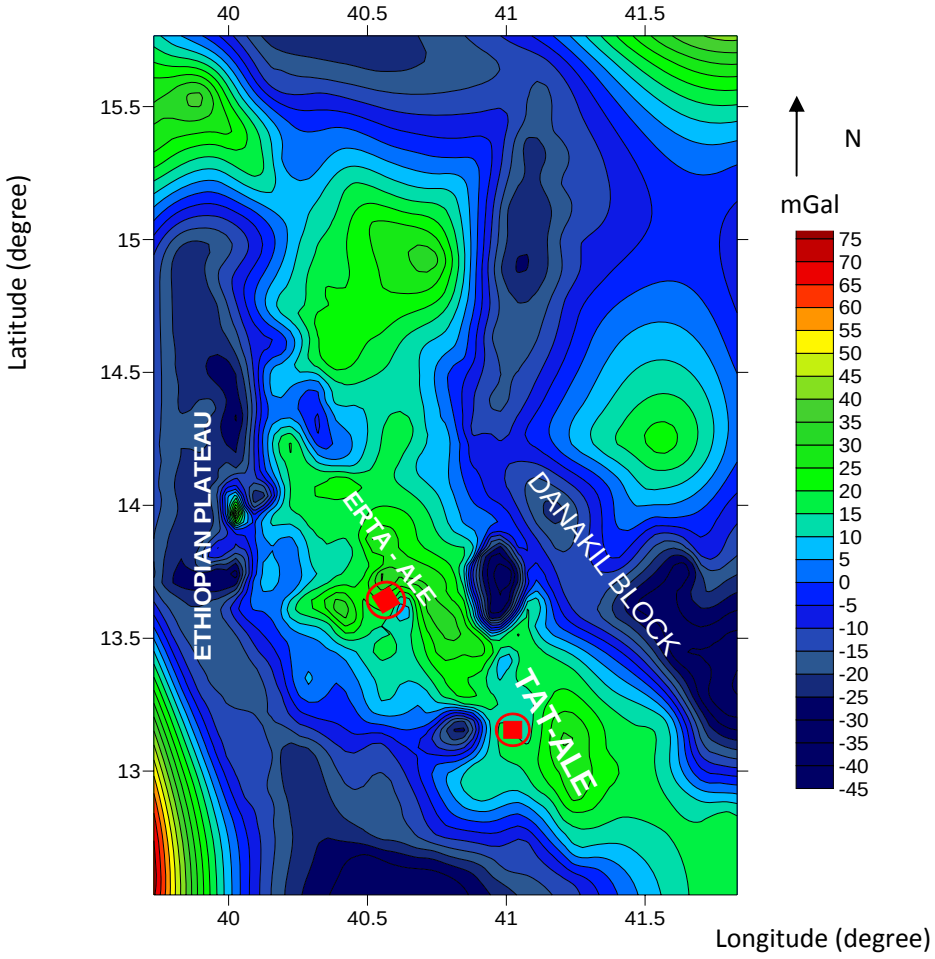

Figure 4.3 Residual Anomaly map

4.2.2.2 Regional gravity anomaly

The regional gravity anomaly map (Figure 4.4), which was extracted from the Bouguer gravity anomaly map shows smoothed large scale regional features. The high regional gravity anomaly is dominated in NW-SE trending, which is parallel to Red Sea and probably related to a NNW-SSE elongated caldera. The map has a range of values between -150mGal and 20 mGal with a contour interval of 5mGal.

The regional anomaly has a higher anomaly at the nearly NNW –SSE and the rest of the region is filled with low regional gravity anomaly. The NNW-SSE trend of the regional anomaly map has similarity with the Bouguer anomaly map at the same location as shown in Figure 4.2. Most of the regional and the Bouguer anomalies have a similarity with respect to the locations where the positive and negative anomalies are found.

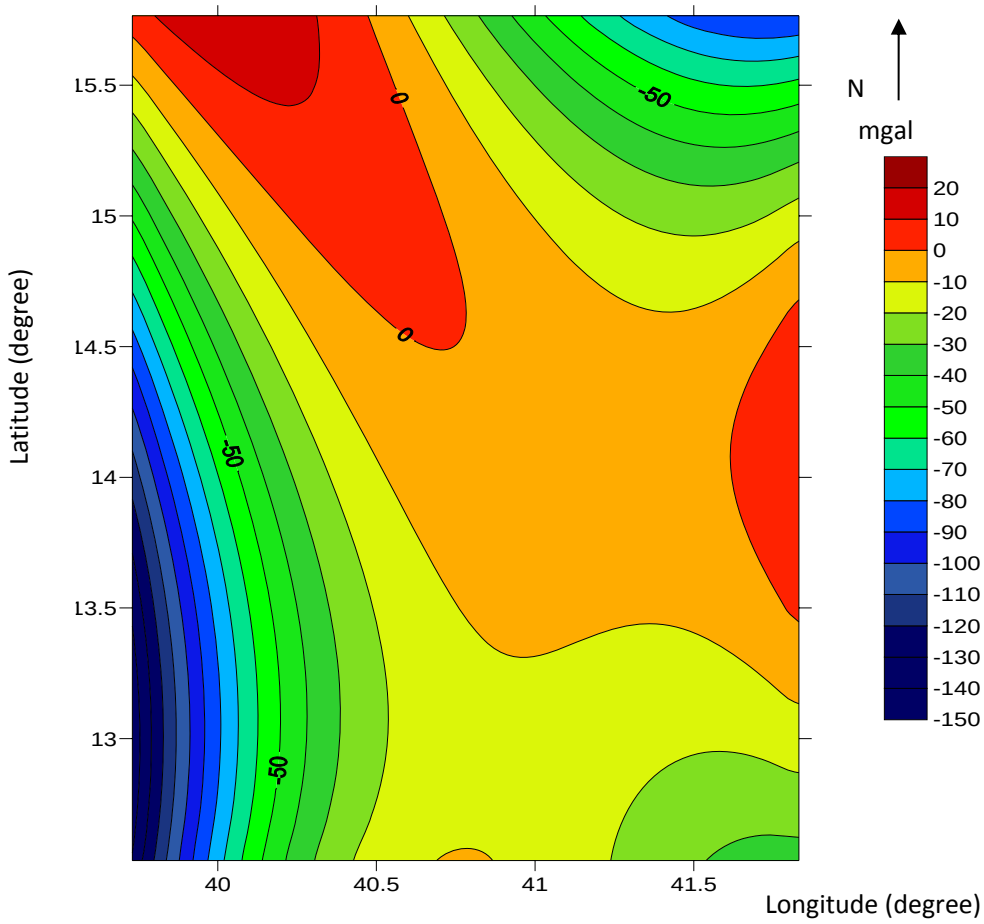

Figure 4.4 Regional Anomaly map

4.3 Data processing

In order to enhance and isolate the gravity anomalies filtering and enhancement techniques are carried out.

4.3.1 Horizontal gradient

The horizontal gradient method has been used intensively to locate contacts of density contrast from gravity data (Cordell, 1979) or pseudogravity data (Cordell and Grauch, 1985). Short-wavelength anomalies are also enhanced. Blakely (1995) stated that the horizontal gradient of gravity anomaly caused by a tabular body tends to overlie the edges of the body if the edges are vertical and well separated from each other. The biggest advantage of the horizontal gradient method was its least susceptibility to the noise in the data because it only required the calculations of the two first-order horizontal derivatives of the field (Phillips, 1998). The amplitude of the horizontal gradient (Cordell and Grauch, 1985) is expressed as:

$$HG = \sqrt{\left(\frac{\partial g}{\partial x}\right)^2 + \left(\frac{\partial g}{\partial y}\right)^2} \quad ,$$

Where ($\frac{\partial g}{\partial x} and \frac{\partial g}{\partial y}$) are the horizontal derivatives of the gravity field in the x and y directions. Horizontal-gradient maxima occur over the steepest parts of potential-field anomalies, and minima over the flattest parts.

The amplitude of the horizontal gradient has been calculated from Bouguer anomaly to locate contacts of density contrast from gravity data in Figure 4.5. High gradient values were observed around the Ethiopian plateau escarpment, Erta Ale and Tati Ale volcanic range. The major faults striking in the N-S direction that dissects the area into the Ethiopian plateau escarpment boundary and the Afar depression can be observed in Figure 4.5. The most interesting result is that the locations of the volcanic ranges are well correlated with the horizontal gradient anomalies, which indicates that the volcanic areas in study area are structurally controlled.

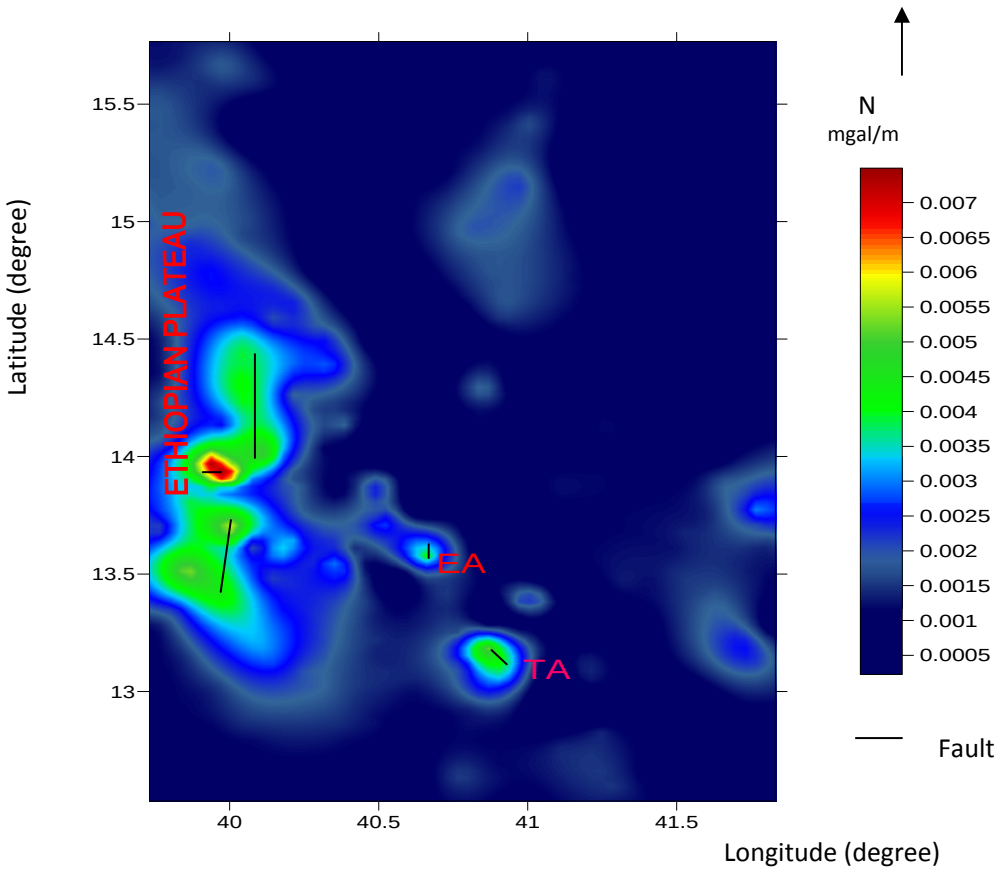

Figure 4.5 Horizontal gradient map.

EA = Erta-Ale, TA = Tat-Ale

4.3.2 Upward continuation

Upward continuation filter is based on the concept that if the gravity values are known anywhere on the earth's surface, gravity at any higher elevation can be calculated from these values this process which has a similar effect as low –pass filter removes short wave lengths and enhances long wave lengths of regional anomalies. The gravity field is upward continued to suppressed higher wave numbers that are related to near surface bodies and this will allow the regional deep seated structure to become clearer.

Upward continuation filtering is carried out (Figure 4.6) on the Bouguer anomaly data at an elevation of 10km, 20km and 30km higher than that at which the Bouguer anomaly is taken . The upward continued Bouguer anomaly illustrates, as elevation increases more of the smaller features and shorter wavelengths disappear.

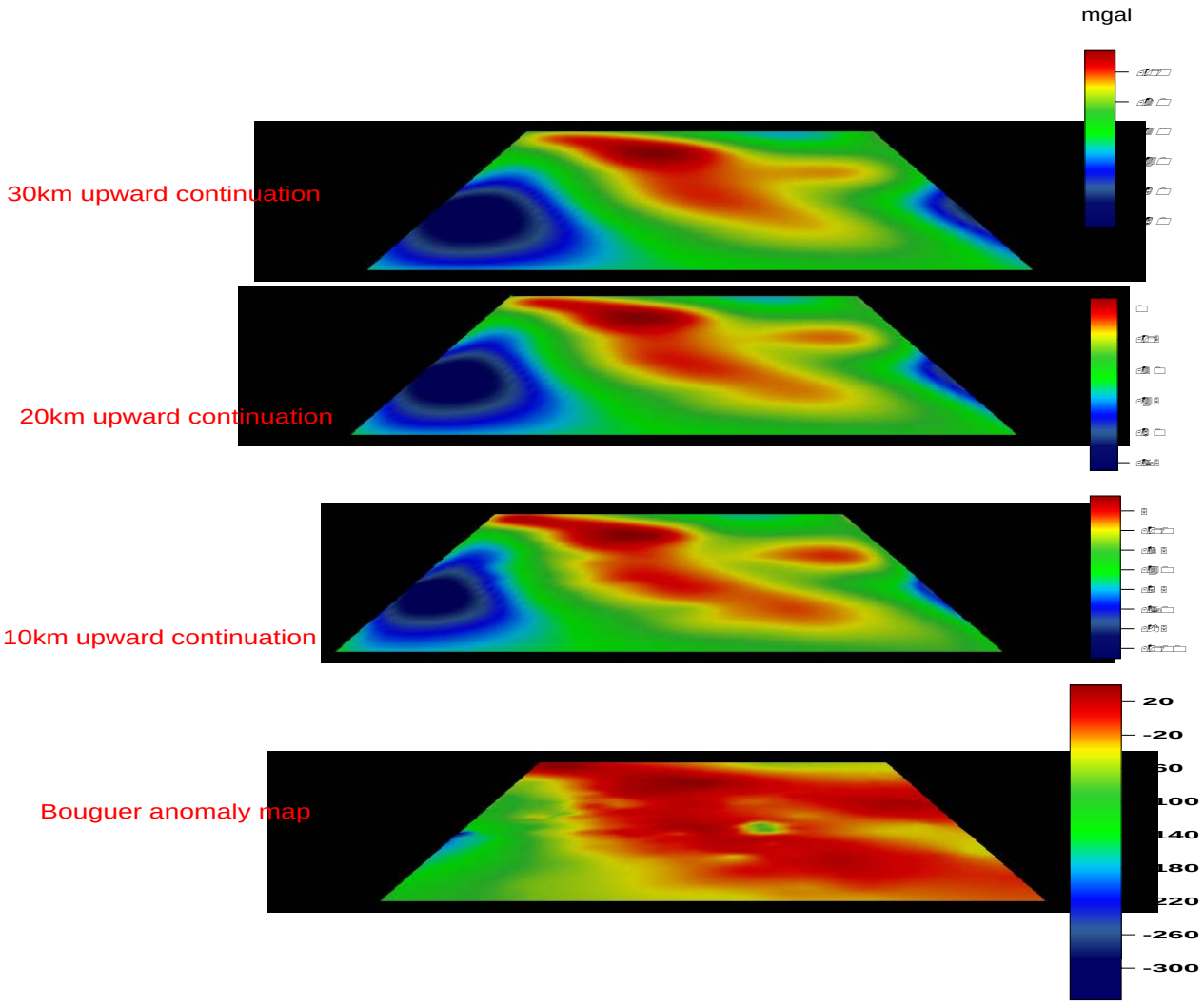

Figure 4.6 upward continuations.

4.4 Euler deconvolution of gravity signal

Euler deconvolution can be usefully applied to gravity data provided that thought is given to the correct Structural Index (SI). 2D form of Euler's equation is expressed as:

$$x_0\frac{\partial T}{\partial x}+y_0\frac{\partial T}{\partial y}+\alpha = x\frac{\partial T}{\partial x}+y\frac{\partial T}{\partial y}+nT$$

Where T -is gravitational field

n -is structure index, which is a measure of the rate change with distance of the field.

The left hand sides contain the unknown source location (x_0, y_0), and unknown constants α. The right hand sides contain the known observation location(x,y).

For determination of depth the Euler Deconvolution method has been applied to the selected profiles using Euler 1.15 software (Cooper, 2000-2004). Several structural indexes are assigned and found that structural index of 0.5 for each profile which gives good clustering solutions. The result of the Euler deconvolution in Figure 4.6 and Figure 4.7 shows the depth to the causative body to be modelled.

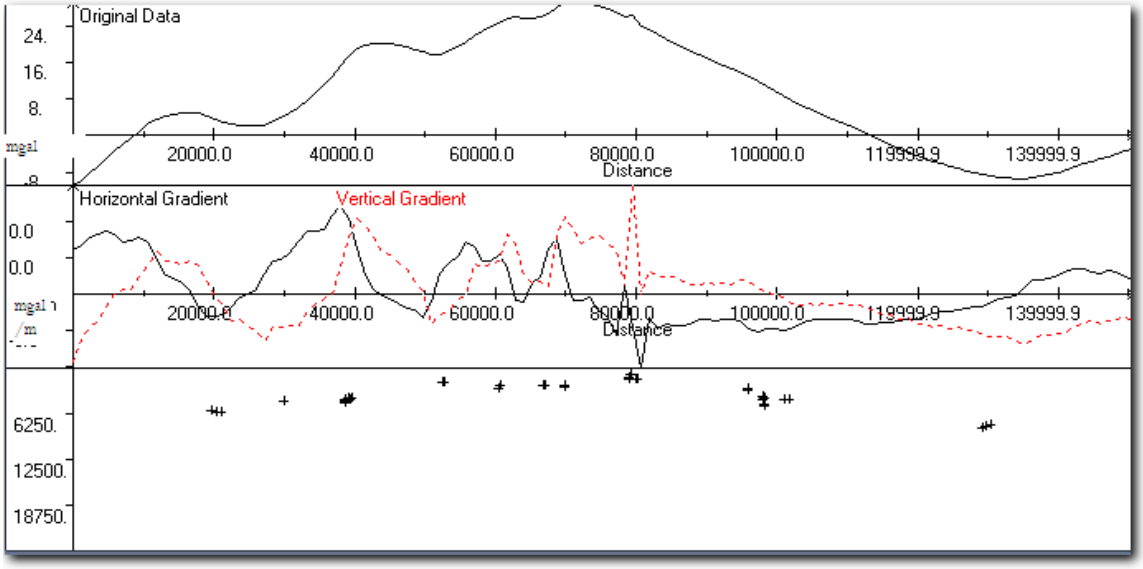

Figure 4.7 Euler deconvolution for profile AA'

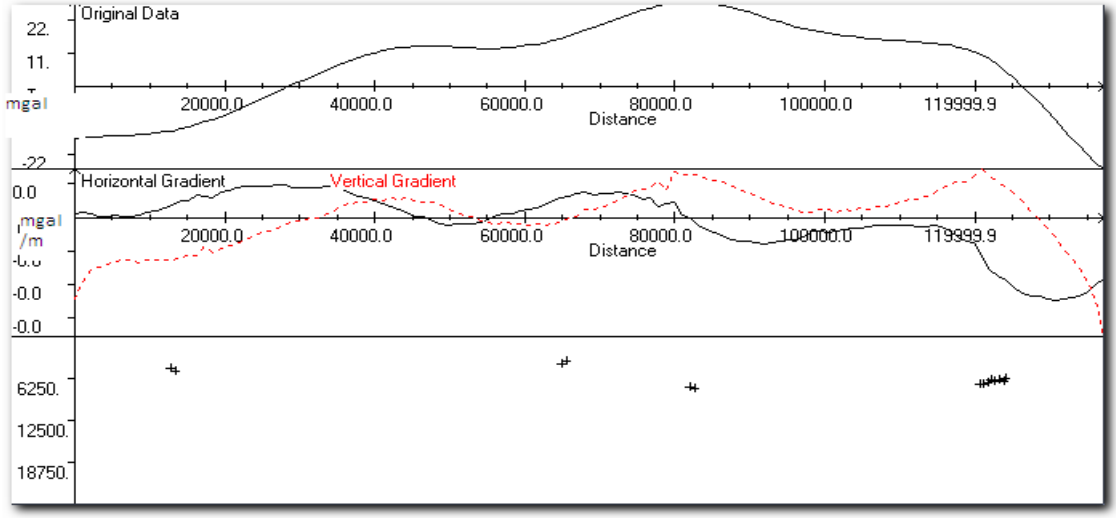

Figure 4.8 Euler deconvolution for profile BB'

CHAPTER 5

GRAVITY MODELLING AND INTERPRETATION

5.1 Gravity modelling

There are many different techniques available to perform the modeling procedure and they can be divided into two main categories:

1. Direct methods, or "forward modelling" These involves setting up a model, calculating the gravity anomaly, comparing it with the observed data and adjusting the model until the data are fit well. The initial model may be obtained using parametric measurements and/or geological.

2. Indirect methods, or “inverse modelling” These involve using the data to draw conclusions about the causative body, e.g., the excess mass, the maximum depth to the top. Some parameters may be calculated, but the full inverse problem i.e., calculating the body from the anomaly, is inherently non-unique.

5.1.1 Initial model

In modelling, geological constraints and geophysical information derived by other methods are necessary. For this reason the seismic wave velocity(V_p)of the study area (Makris and Ginzburg, 1987) which was converted to densities using velocity/density relationships, $\rho=0.252 +0 .3788V_p$ (Christensen and Mooney, 1995) and Euler Deconvolution discussed in previous chapter were used as initial density (Table 5.1) and depth determination respectively.

Crustal layer	V_p(km/s)	ρ (kg/m^3)	Depth (km)
Unconsolidated sediments and Pyroclatic	4.1	2350-2560	3-4
Upper crust	6.1-6.45	2600-2700	7-11
Lower crust	6.6-7.2	2800-2980	15-19
Upper mantel	7.4-7.8	3100-3200	15-22

Table 5.1 P-wave velocity and density obtained from Makris and Ginzburg’s (1987)

5.1.2 2.5-D Forward modelling

The most common technique in gravity modelling is computer forward modeling of polygonally-shaped, multiple 2- and 2.5-D bodies (Cady, 1980) along profiles of data. The difference between 2- and 2.5-D is that for 2.5-D bodies, the cross-sectional shape extends out a finite distance (called strike lengths) in both directions perpendicular to the profile.

The 2.5-D forward gravity modeling was constructed using 'Grav2dc' software (Cooper, 2003a, b) and the programs are based on the Talwani algorithm to calculate anomalies (Talwani et al., 1959). The background density which was used in modelling is density contrast between the body and 2.67gm/cm^3. Two profile (Figure 5.1) lines were chosen for modelling to illustrate the subsurface signature of the residual gravity anomaly.

Profile AA′

This profile is extending over a horizontal distance of 140 km in the NE-SW direction and runs over Erta Ale volcanic range (Figure 5.1). Showing the residual anomaly to be ranging from -10.75 mGal to 31.5mGal. A best fit between calculated and observed anomalies consist of five layers and two fragment material beneath the profile in Figure 5.2.

Profile BB′

This profile traverses entirely over Tat Ale volcanic range shown in Figure 5.1.It has a total horizontal length of 135 km where the anomaly varies between -27.56 to 29.01 mGal. A best fit between calculated and observed anomalies consist of five layers and two fragmented material beneath the profile. This best fit model for the residual anomaly and corresponding computed anomaly are presented in Figure 5.3.

5.2 Interpretation of the modeled layer

The interpretations of the above models have been made separately in order to have a better picture for the anomalies which are exhibited in the residual gravity anomaly map.

1. **Model of profile AA'**

   This model indicates:-

- The presence of low density material with density 2.45g/cm^3 can be interpreted as a Mesozoic sedimentary rock with a maximum thickness of 4.6 km.

- The presence of high density material density 3.0g/cm^3 can be interpreted in terms of intrusive body into the crust or the thinning of crust. The depth to the top of the intrusion is 14.65km near to Erta Ale volcanic range. The interpretation is consistent with Makris and Ginzburg (1987) view of the crust below this region is only 14 Km.
- The two fragmented low density bodies are related to quaternary sediment.

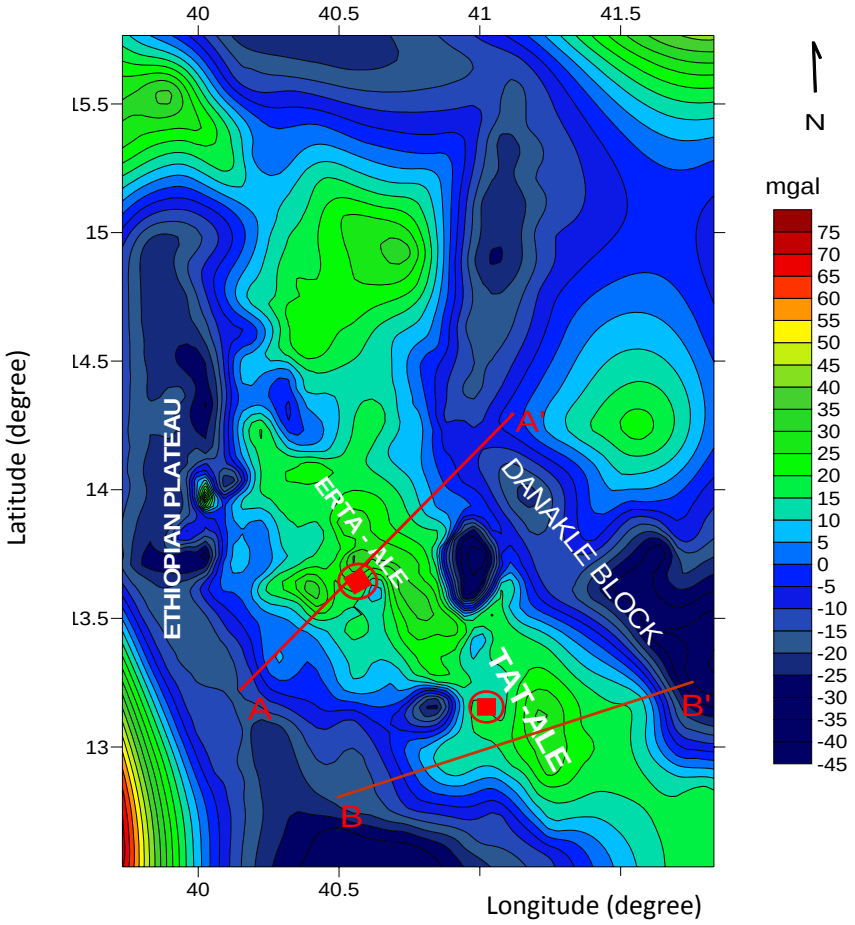

Figure 5.1 Profiles location on the residual Anomaly map.

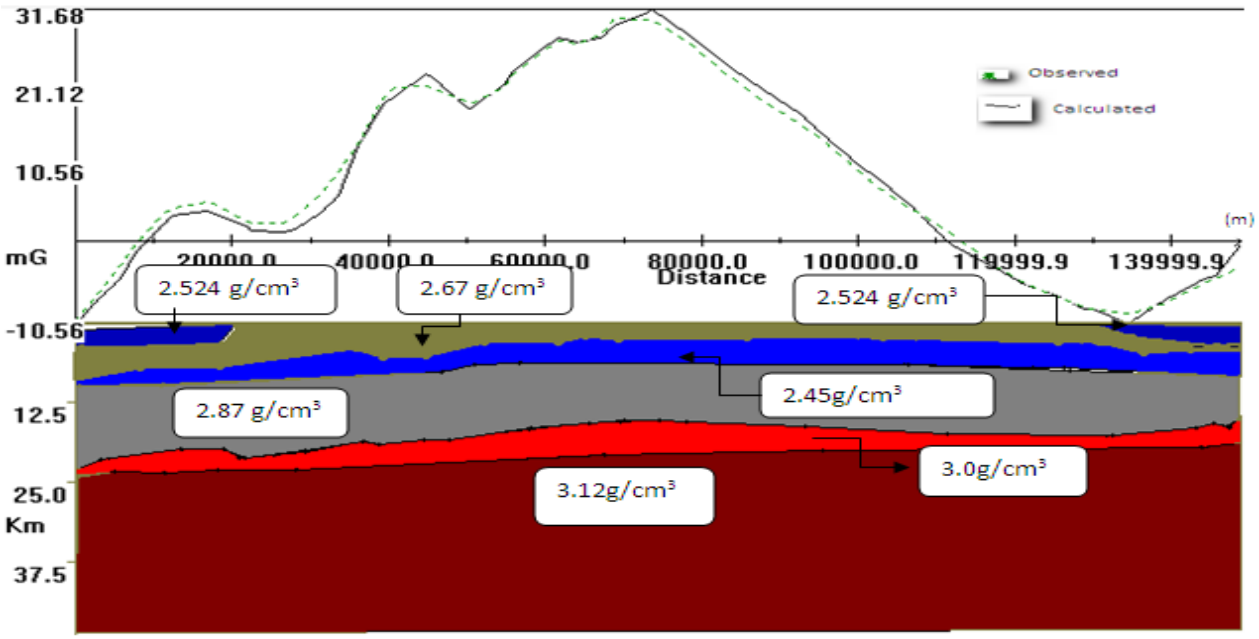

Figure 5.2 The 2.5D forward modelling along profile AA′

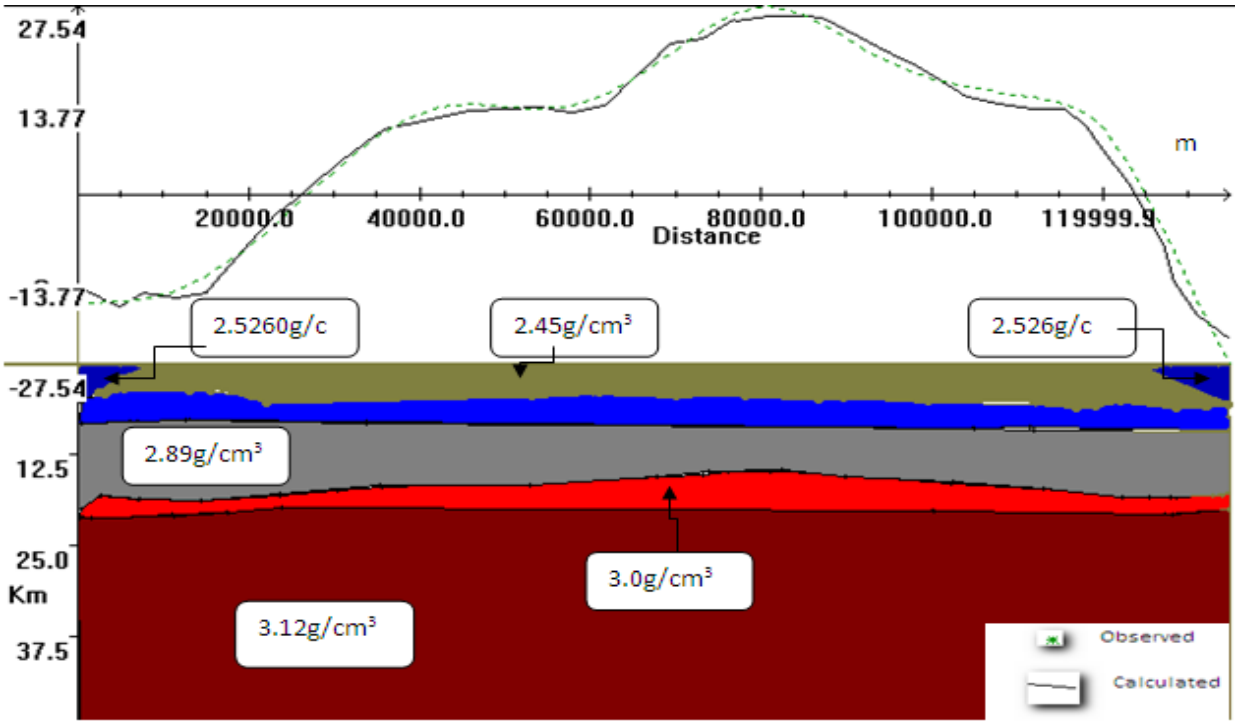

Figure 5.3 The 2.5D forward modelling along profile BB′

2. Model of profile B-B'

This model indicates:-

- The presence of low density material density 2.45g/cm^3 again related to Mesozoic sedimentary with a maximum thickness of 4.3km.
- The presence of high density material density 3.0g/cm^3 can be interpreted in terms of intrusive body into the crust or the thinning of crust or the thinning of crust. The depth of the top of intrusion 14.75km.This result is also agrees with Makris and Ginzburg(1987) view of the crust below this region is only 14 Km.
- The two fragmented low density bodies are correlated to sediments.

CHAPTER 6

6. CONCLUSIONS AND RECOMMENDATIONS

6.1 Conclusions

From this study one can conclude;

Residual gravity anomaly maps show that a narrow zone within the area is dominated by gravity maxima that occur of the Erta Ale and Tat Ale magmatic segments.

- The high gradient in the residual gravity anomalies depicted the existence of geological structures /contact, fault/. The high gradient residual gravity anomalies that are found in the Ethiopian plateau escarpment, Eta Ale and Tat Ale area are an indication of the existence of some geological structures in the area. These high gradient steep residual gravity anomalies are an indication of a Fault/contact/.
- The Ethiopian Plateau and Danakil block are filled with negative residual anomaly implying there is low density material beneath the surface .This will agree with (Mohr, 1967a) the northern part of the Danakil horst is composed of Precambrian basement rocks overlain by Mesozoic sedimentary rocks similar to those on the Ethiopian Plateau.
- The results of the 2.5D forward modelling of residual gravity profiles reveal that the thickness of the crust is 14.4 km near to the volcanic ranges and the existence of the Mesozoic sedimentary rocks beneath the study area.

6.2 Recommendations

Based on the investigations made under this study the following recommendations are forwarded.

- More detail integrated geophysical work such as refraction seismic should be conducted for further study.
- The modelling result with a significant thickness of Mesozoic sedimentary rock can be a potential exploration target for petroleum exploration.

References

Almond, D.C., 1986. Geological evolution of the Afro-Arabian dome. Tectonophysics 331, 302–333.

Barberi, F., Varet, J., 1975. Recent volcanic units of Afar and their structural significance. In: Pilger, A., Rosler, A. (Eds.), Afar Depression of Ethiopia, Proceedings of an International Symposium on the Afar Region and Rift

Bergzabren, Germany, 1974, vol. **1**. E. Schweizerbart_sche Verlagsbuch hand lung, Stuttgart, Germany, pp. 174–178.

Barberi, F., Varet, J., 1977. Volcanism of Afar: small-scale plate tectonics implication. *Geological Society of America Bulletin* 88, 1251–1266.

Barberi, F., Borsi, S., Ferrarea, G., Marinelli, G., Santcroce, R. Tazief, H., Varet, J., 1972. Evolution of the Danakil Depression(Afar Ethiopia) in light of radiometric age determination. *Journal of Geology* 80, 720–729.

Barberi, F., Bonati, E., Marinelli, G., Varet, J., 1974. Transverse tectonic during the split of continent: Data from the Afar rift.Tectonophysics 23, 17–19.

Berhe, S.M., Desta, B., Nicoletti, M., Teferra, M., 1987. Geology, geochronology and geodynamic implications of Cenozoic magmatic province in W and SE Ethiopia. *Journal of The Geological Society of London* 144, 213–226.

Black, R., Morton, W.H., Hailu, T., 1974. Early structure around the Afar triple junction. *Nature* 248, 496–497.

Blackly, R. J., 1995, Potential theory in gravity and magnetic applications: Cambridge Univ. Press.

Bosworth , W., McClay, K., 2001. Structural and stratigraphic evolution of the Gulf of Suez Rift, Egypt: a synthesis. Memoires due Museum National dltistorire nationalle 186, 567– 606.

Bosworth, W., Strecker, M.R., 1997. Stress field changes in the Afro-Arabian Rift system during the Miocene to recent period.

Civetta, L., DeFino, M., Gasparini, P., Ghiara, M.R., LaVolpe, L. Lirer, L., 1975. Geology of central-eastern Afar (Ethiopia). In:Pilger, A., Rosler, A. (Eds.), Afar Depression of Ethiopia,

Cordell, L., 1979, Gravimetric expression of graben faulting in Santa Fe Country and the Espanola Basin, New Mexico: New Mexico. Geol. Sot. Guide book, 30th Field Conf., 59-64.

Cordell, L., and Grauch, V. J. S., 1985, Mapping basemen magnetization zones from aeromagnetic data in the San Juan Basin, New Mexico, in Hinze, W. J., Ed., The utility of regional gravity and magnetic anomaly maps: Sot. Explor. Geophys., 181and197.

Collet, B., Taud, H., Parrot, J.F., Bonavia, F., Chorowicz, J., 2000. A new kinematic approach for the Danakil Block using a digital elevation model representation. Tectonophysics 316, 343–357.

Cooper, G.R.J., (2003a). Grav2dc, V.2.10 for Microsoft windows. School of Geosciences University of the Witwatersrand, Johannesburg, South Africa [Online]. [Accessed 19th May 2009*]. www.cooperg@geosciences.witz.ac.za*

Courtillot, V.E., 1980. Opening of the Gulf of Aden and Afar by progressive tearing. Physics of the Earth and Planetary Interiors 21,343–350.

Courtillot, V., 1982. Propagating rifts and continental breakup.Tectonics 1, 239–250.

Courtillot, V., Achache, J., Landre, F., Bonhommet, N., Montigny, R., Feraud, G., 1984. Episodic spreading and rift propagation; new paleomagnetic and geochronologic data from the Afar nascent passive margin. Journal of Geophysical Research 89, 3315–3333.

Courtillot, V., Armijo, R., Tapponnier, P., 1987. Kinematics of the Sinai triple junction and a two-phase model of Arabia–Africa rifting continental extensional tectonics. Geological Society Special Publications 28, 559–573.

DOBRIN, M.B., AND SAVIT, C.H., 1988; Introduction to Geophysical Prospecting. McGraw – Hill Inc. Singapore

Ebinger, C.J., Casey, M., 2001. Continental breakup in magmatic provinces: an Ethiopian example. Geology 29, 527–530.

Ebinger, C.J., Sleep, N.H., 1998. Cenozoic Magmatism throughout East Africa resulting from impact of a single plume. *Nature* 395,788–791.

Ebinger, C.J., Yemane, T., WoldeGabriel, G., Aronson, J.L., Walter, R.C., 1993. Late eocene-recent volcanism and faulting in the southern Main Ethiopian Rift. Journal of the Geological Society of a London 150, 99–108.

Ghebreab, W., 1998.Tectonics of the Red Sea region reassessed. Earth Science Reviews 45, 1–44.

Ghebreab, W., Carter, A., Hurford, A.J., Talbot, C.J., 2002.Constraints for timing of extensional tectonics in the western margin of the Red Sea in Eritrea. Earth and Planetary Science Letters 200, 107–119.

Hofmann, C., Courtillot, V., Feraud, G., Rouchett, P., Yirgu, G., Ketefo, E., Pik, R., 1997.

Timing of the Ethiopian flood basalt Makris, J., Ginzburg, A., 1987. The Afar Depression; transition between continental rifting and sea-floor spreading. Tectonophysics 141, 199–214.

Kazmin, V.G., Byakov, A.F., 2000. Magmatism and crustal accretion in continental rifts. *Journal of African Earth Sciences* 30, 555–568.

McKenzie, D.P., Davis, D., Molnar, P., 1970. Plate tectonics of the Red Sea and East Africa. *Nature* 226, 243–248.

Montenat, C., Ott d_Estevou, P., Purser, B.H, 1998. The Suez Rift and the north-western Red Sea Neogene sedimentation and tectonic evolution. In: Purser, B.H. (Ed.), Dynamics and Methods of Study of Sedimentary. Oxford and IBH Publishing Company, New Delhi, India, pp. 173–199.

Mickus.k .: 2006 Gravity analysis of the main Ethiopian rift. *Journal of African Earth Sciences* 48 (2007) 5969.

Mickus, K. L., and Peeples, W. J., 1992; Inversion of gravity and magnetic data for the lower surface of a 2.5 dimensional sedimentary basin: Geophysical Prospecting, 40, pp. 171-194.

Mohr, P.A., 1975. Structural setting and evolution of Afar. In: Pilger, A., Rosler, A. (Eds.), Afar Depression of Ethiopia, Proceedings of an International Symposium on the Afar Region and Rift Related Problems, Bad Bergzabren, Germany, 1974, vol. **1**. E.Schweizerbart_sche Verlagsbuchhandlung, Stuttgart, Germany, pp.27–37.

Moritz, H., 1971; Geodetic References System 1967. Pub. No. 3, *Bulletin Geodesique*, Paris.

Moritz, H., 1984; Geodetic Reference System 1980. In: C.C. Tscherning (ed), The Geodesist's Handbook 1984 – Bull.Geod. 58, 388-398

Nagy D. 1966; The gravitational attraction of a right rectangular prism. Geophysics

Pallister, J.S., 1987. Magmatic history of Red Sea rifting; perspective from the central Saudi Arabian coastal plain. *Geological Society of America Bulletin* 98, 400–417.

Phillips, J.D., 1998, Processing and Interpretation of Aeromagnetic Data for the Santa Cruz Basin-Patahonia Mountains Area, South-Central Arizona: U.S. Geological Survey Open-File Report 02-98.

Purcell, P.G., 1976. The Marda Fault Zone, Ethiopia. *Nature* 261, 569–571.

Robinson, E., and Caruh, C., 1988; Basic exploration geophysics: Wiley and Sons.

Sultan, M., Becker, R., Arvidson, R.E., Shore, P., Stern, R.J., El Alfy, Z., Guinness, E.A., 1992. *Nature* of the Red Sea crust: a controversy revisited. Geology 20, 593–596.

Telford, W.M., Geldart, L.P., and Sheriff, R.E., 1990; Applied Geophysics, Cambridge Univ. Press.

Torge, W., 1989; Gravimetry, Walter de Gruyter and Co. Berlin, Germany.

Talwani, M, Worzel, JL, and Landisman, M., 1959. Rapid Gravity Computations for Two-Dimensional Bodies with Application to the Mendocino Submarine Fracture Zone, *Journal of Geophysical Research*, 64, 49-61.

Tefera, M., Chernet, T., Haro, W., 1996. Explanation of the Geological Map of Ethiopia. Ethiopian Institute of Geological Surveys, Addis Ababa, vol. **3**, p. 79.

Vail, J.R., 1985. Pan-African (late Precambrian) tectonic terranes and reconstruction of the Arabian–Nubian Shield. Geology 13, 839– 842.

Varet, J., 1978. Geology of Central and Southern Afar (Ethiopia and Djibouti Republic) F. Gasse for Chapter IV on Sedimentary Formation. Eds. CNRS, France, Paris, p. 118.

Vellutini, P., 1990. The Manda-Inakir Rift, Republic of Djibouti: a comparison with the Asal Rift and its geodynamic interpretation. Tectonophysics 172, 141–153.

White, R., McKenzie, D., 1989. Magmatism at rift zones; the generation of volcanic continental margins and flood basalts. *Journal of Geophysical Research* 94, 7685–7729.

DECLARATION

The thesis is my original work, has not been presented for a degree in any other university and that all sources of materials used for the thesis have been duly acknowledged.

Name _____

Signature _____

Date _____

This thesis has been submitted for examination with my approval as university advisor.

_____	_____	_____
Advisor	Signature	Date